ISSN 1392 - 1207. MECHANIKA. 2011. 17(4): 395-399

Analysis of cylindrical piezoelectric actuator used in flow control device

R. Bansevičius*, R. Rimašauskienė, D. Mažeika***, G. Kulvietis******

**Kaunas University of Technology, K. Donelaičio 73, 44029 Kaunas, Lithuania, E-mail: ramutis.bansevicius@ktu.lt*
***Kaunas University of Technology, K. Donelaičio 73, 44029 Kaunas, Lithuania,*
E-mail: ruta.rimasauskiene@gmail.com
****Vilnius Gediminas Technical University, Saulėtekio al. 11, Vilnius, 10223, Lithuania, E-mail: dalius.mazeika@vgtu.lt*
*****Vilnius Gediminas Technical University, Saulėtekio al. 11, Vilnius, 10223, Lithuania,*
E-mail: genadijus.kulvietis@vgtu.lt

1. Introduction

Piezoelectric actuators are widely used for high precision mechanical systems such as positioning devices, manipulating systems, control or flow control equipment and etc [1 - 3]. Piezoelectric actuators have advanced features such as high resolution, short response time, compact size, and good controllability [1, 2, 4]. Many design principles of piezoelectric actuators are proposed and used [5]. Summarizing its all the following types of piezoelectric actuators can be specified: traveling wave, standing wave, hybrid transducer, and multimode vibrations actuators [2, 6].

Demand of new displacement transducers that can achieve high resolution and accuracy of the driving object increases in nowadays. Piezoelectric actuators have advanced features compare to others and are widely used for different commercial applications [1, 6]. A lot of design and operating principles are investigated to transform mechanical vibrations of piezoceramic elements into elliptical movement of the contact zone of actuator [2, 4, 7]. However summarizing its all the following types of piezoelectric actuators can be specified - traveling wave, standing wave, hybrid transducer, and multivibration mode [5, 8]. Traveling wave piezoelectric actuators fall under two types – rotary and linear. Rotary type actuators are one of the most popular because of high torque density at low speed, high holding torque, quick response and simple construction. Linear type traveling wave actuators feature these advantages as well but development of these actuators is complex problem [9]. Usually elastic beam is used as the main part of linear traveling wave actuator design and traveling wave oscillations are generated on it [5, 6].

Traveling wave piezoelectric actuator which type is rotary is studied numerically and experimentally in this paper. This acting method of the actuator allows using it in the flow control systems.

2. Design of flow control device

The flow control device construction, which is analyzed in the paper, in practice can be adapted in various areas: in the laser beam, gas, liquid or light flow control systems. The scheme of this flow control device presented in Fig. 1 has been developed and patented [10] at Kaunas University of Technology.

The flow control device consist of cylindrical body *1*, mounting ring *2* is rigidly entrenched in it. This ring *2* is used like a support of piezoceramic actuator (cylinder) *3*. On the piezoceramic actuator *3* is loaded mounting ring *4* of the plate with a pad. The plate *5* with micropores or notches is glued on the mounting ring *4*. Another mounting ring *7* is threaded and plate *6* is rigidly entrenched on it, then both of them are screwed on the cylindrical body *1*. A center tab *8* fastened on cross-plates, and their mutual compression is adjusted on mounting ring *7* threaded support. From the plates (with micropores or notches) *5* and *6* is formed the flow permeability regulating membrane.

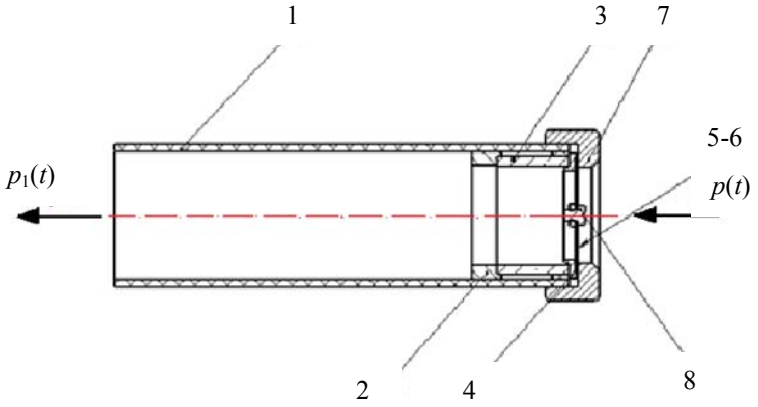

Fig. 1 The flow control device: *1* – cylindrical body; *2* – mounting ring; *3* – piezoelectric actuator (cylinder); *4* – mounting ring of the plate with a pad; *5* – plate; *6* – plate; *7* – threaded mounting ring; *8* – center tab

The principle of operation can be explained as follow. Traveling deformation waves are generated on piezoceramic actuator (cylinder) *3* and mounting ring *4* with glued plate *5* in contact with the actuators output link can be rotated by the clockwise direction or against it.

During the initial operation at the time of the plate *5* and *6* is geometrically adjusted so that the adjacent micropores or notches do not overlap and flow control membrane permeability would be minimal or zero. Optical moiré interference pattern is generated as the geometric location of the adjacent micropores or notches of the two plates change when one of the plates rotates. This interference effect alters the flow permeability. When piezoceramic actuator gets signal, it generates traveling deformation waves and optical Moiré interference pattern is generated between two plates *5* and *6*.

In cases where the membranes are made up of plates of round or hexagonal micropores contained in a regular rectangular or shifted array of nodes, permeability is maximized when the optical Moiré interference generated and overlaps of the micropores in Moiré circles is the greatest possible amount. This may be precisely and quickly heated liquids or gases microflow control. This device can be applied to drug dosing, and others.

3. Design and operating principle of piezoelectric actuator

Sinusoidal voltage with the phase shift by $\pi/3$ is applied on each piezoceramic element.

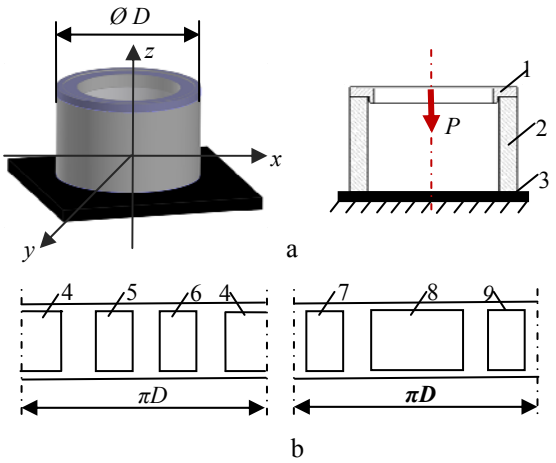

Fig. 2 Piezoceramic cylinder with a steel ring: a) general scheme, b) evolvents of a cylindrical inner and outer surfaces (single phase). *1* – steel ring, *2* – piezoelectric cylinder with electrodes formed on the outer and inner surfaces of the cylinder, *3* – vibrations depressant substance, *4-9* – electrode configurations

Operating principle of the actuator is based on the modified first way described in Section 1 of this paper. Travelling wave is generated in the upside beam when mechanical harmonic forces from piezoceramic plates are applied and actuator starts to vibrate. Excitation frequency near 4th flexural mode of upside beam is used. Due to height difference between up and down sides, the downside beam oscillates on 2nd flexural mode at the same frequency (Fig. 2, b). Phase difference between oscillations of the ends of upside and downside beams appears when excitation frequency is close to resonance. Therefore one end of the upside beam is excited while another is damped and travelling wave oscillations without reflection are obtained. Travelling wave motion is illustrated at four points in time during the vibration period of the actuator (Fig. 3).

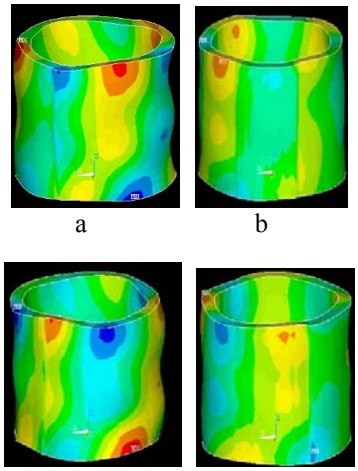

Fig. 3 Vibration of cylindrical actuator under 3-phase excitation voltage at four time steps: a) $t = 0$; b) $t = \frac{1}{2}\frac{\pi}{\omega}$; c) $t = \frac{\pi}{\omega}$; d) $t = \frac{3}{2}\frac{\pi}{\omega}$

4. Results of numerical modeling

Numerical modeling of piezoelectric actuator was performed to validate actuator design and operating principle through the modal and harmonic response analysis. FEM software ANSYS 10.0 was employed for simulation. FEM model (Fig. 4) was built and the following materials were used for actuator modeling: bronze was used for the oscillator and piezoceramic PZT-8 was used for piezoelements.

Modal analysis of piezoelectric actuator was performed to find proper resonance frequency. Material damping was assumed in the finite element model. No structural boundary conditions were applied. Examining results of modal analysis it was determined that vibration mode No. 71 (61 kHz) is exploitable for further investigation.

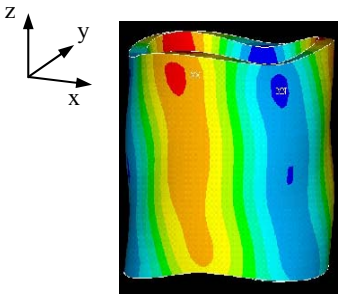

Fig. 4 Finite element model of the cylindrical actuator and vibration mode of the actuator at 61 kHz

Harmonic response analysis was performed with the aims to find out the actuator's response to sinusoidal voltage applied on electrodes of the piezoceramic elements, to verify the operating principle. Analyzing oscillation characteristics travelling wave vibrations on the upside cylinder of the actuator will be manifested. Excitation scheme of the electrodes was used as shown in Fig. 2, b. A

60 V AC signal was applied. A frequency range from 50 to 70 kHz with a solution at 0.25 kHz intervals was chosen and adequate response curves of upper points' oscillation amplitudes and components were calculated.

Graphs of oscillation amplitudes of the upper contact points indicate that resonant oscillations are obtained at 61 kHz. Fig. 5 illustrates global displacements and their components of upper points of the cylinder.

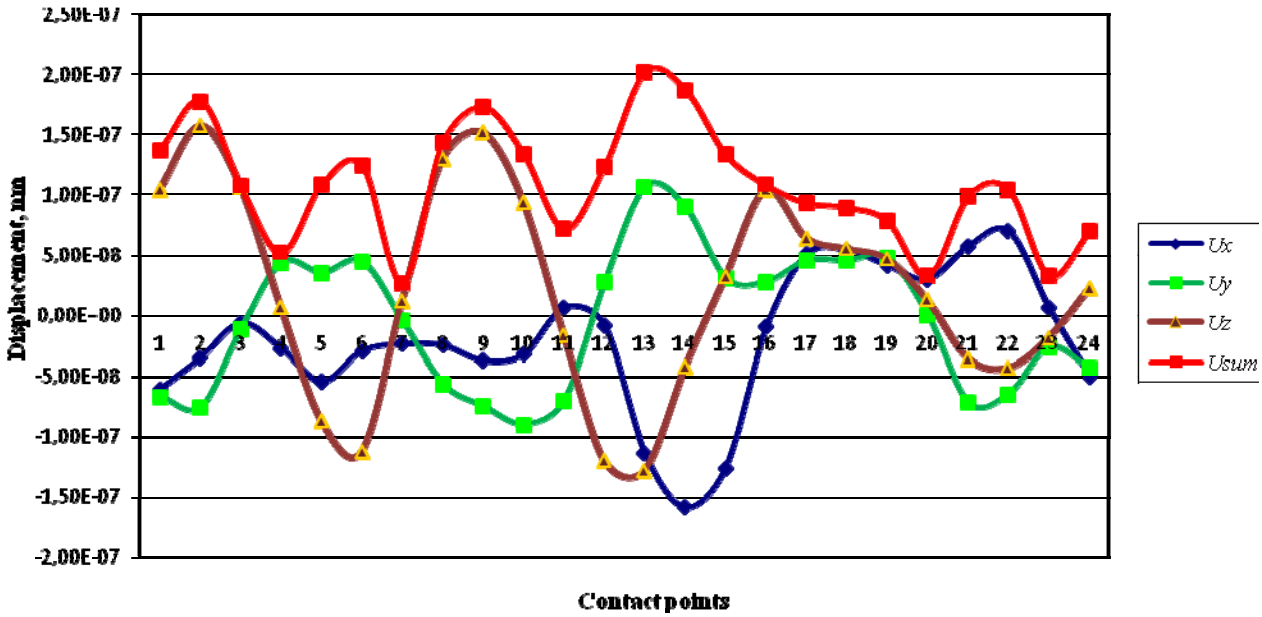

Fig. 5 Global displacements and their components of upper points of cylinder

5. Experimental study of cylindrical actuators' dynamic characteristics

Experiments were carried out to find voltage and frequency, which will let to achieve the largest output link's shift of piezoelectric actuators (cylinder) and validate results of numerical simulation.

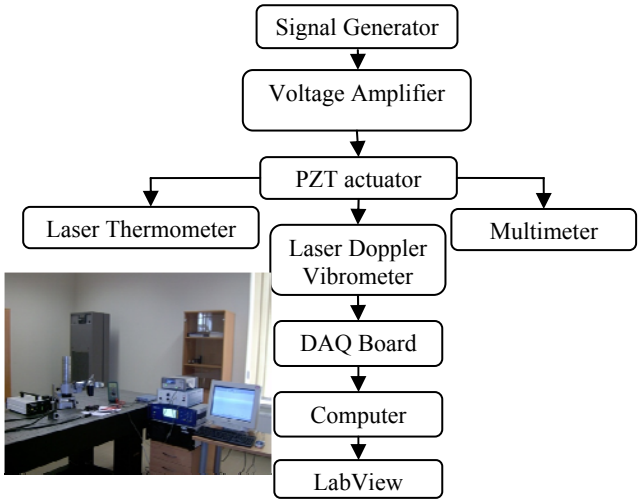

Fig. 6 Experimental stand for the measurement of cylindrical piezo actuator's dynamic characteristics

In order to determine these parameters were carried out experiments by using an experimental stand (Fig. 6), which consists of a programmable signal generator (Aligent 33220, 20 MHz), high voltage amplifier (1 - 150 kHz frequency zone), multimeter (Mastech 8218), laser doppler vibrometer PolytecTM (V_{max} = 10 m/s, frequency zone 0.5 Hz - 1.5 MHz; resolution from 0.1 to 2.5 (mm/s)/√Hz), analog capture card (National Instruments PCI 5102, 20 MS/s) and a computer with installed with LabView software.

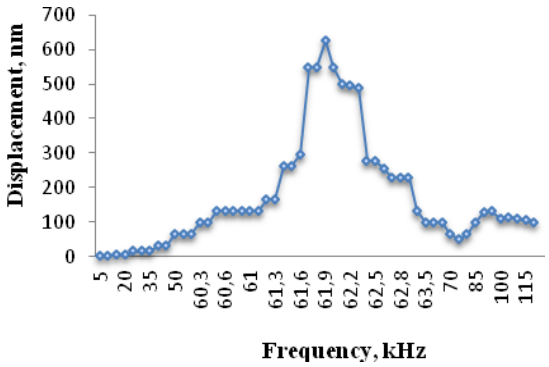

Fig. 7 Dependence of the displacement from the frequency (voltage 10 V)

For the collection and processing of measurement data a specific program in LabView graphical programming environment was designed allowing to receive the amplitude frequency characteristics of the experimental output link.

Using laser vibrometer PolytecTM and computer with specially made LabView program the dependence of shift on frequency was found. During experimental the excitation voltage 10 V was kept constant, the frequency was variable and the shift of piezoelectric actuator's output link was measured.

From the dependence (Fig. 7) can be seen that the greatest displacement improvement is achieved when the frequency is resonant (61.83 kHz).

Once the main resonant frequency is obtained then the maximum displacement of the excitation voltage is 10 V, the displacement dependence on excitation voltage can be determined. In the graphic shown in Fig. 8 can be seen the dependence of the displacement on excitation voltage when the resonant frequency is 61.83 kHz.

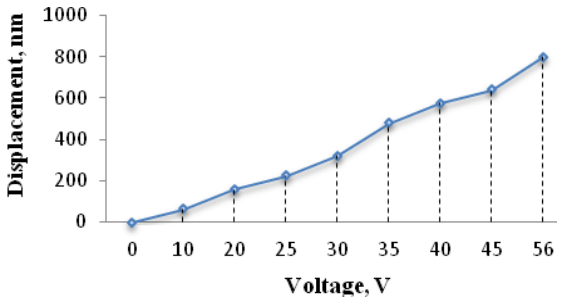

Fig. 8 The dependence of the displacement on excitation voltage when the resonant frequency is 61.83 kHz

From the theory is known that the best mechanical and piezoelectric properties of piezo ceramics are kept when it is working up to 60°C. Therefore, the experiment was continued by keeping the excitation voltage at 56 V.

From the dependence (Fig. 8) it can be seen that while the excitation voltage is 56 V the maximum displacement can be obtained. It means that using this voltage the actuator‘s output link performs the necessary shift in the shortest period of time and turns the steel ring with the plate. Therefore, further experiments have been carried out at such an excitation voltage.

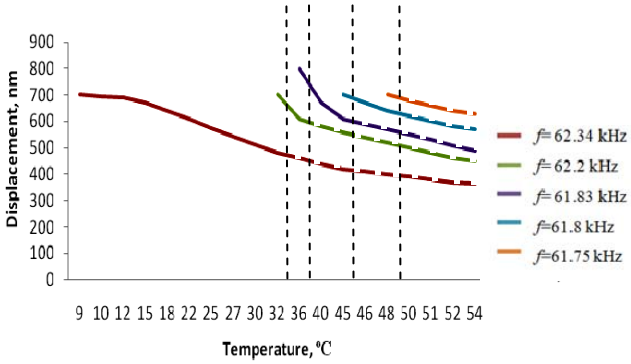

Fig. 9 Dependence of the displacement on temperature by changing the excitation frequency (U = 56 V)

During the experiment with a laser thermometer "Testing 825" the temperature of the output link in piezoelectric actuator (cylinder) was measured. In the dependence (Fig. 9) can be seen that the piezoelectric actuators (cylinder form) begins to operate when it’s first resonant frequency, which gives the maximum output of the link shift (700 nm), is 62.34 kHz. Then the experimental stand was readjusted and found the new frequency (62.2 kHz) at which the displacement of the output link rose again to 700 nm. In this case the five frequencies at which the maximum displacement is obtained at that temperature were found.

From the shift dependence of the temperature (Fig. 9), it can be seen that the maximum output displacement of the link is obtained about 800 nm, when the frequency is 61.83 kHz. This frequency is the most appropriate for the actuator of flow control device and further experiments were carried out at this frequency.

From the dependence (Fig. 9) it can be seen that after a certain period of time the output link of piezoelectric actuators, which is working at specific resonance mode, is reached a temperature of 48°C and then the temperature is raising slowly. According to the characteristics of piezo ceramics it is known that it can operate at such temperatures. Therefore, in this case the frequency of 61.83 kHz is a suitable operating frequency.

Dependence of the experimental excitation frequency on temperature is shown Fig. 10. After completing the experiment, it can be said that with rising the temperature the excitation frequency is decreasing.

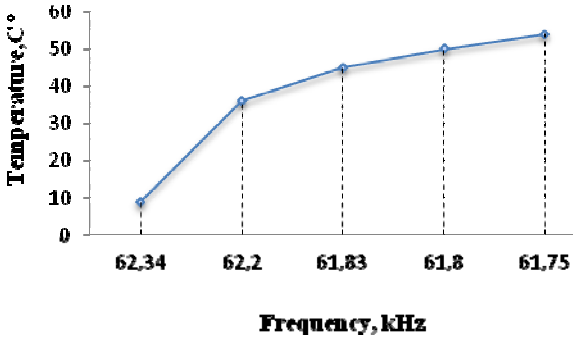

Fig. 10 Frequency dependence on temperature (U = 56 V)

Using the same experimental stand (Fig. 6) the resolution of the flow control device with piezoelectric actuators (cylinder shape) was found. Displacements of the reference point were measured in the following way: on an output link of piezoelectric cylinder was fitted a steel ring, in which a plate with micropores was fixed tightly. The some piece was fixed on steel ring as the starting point. The measurement data was collected and processed by LabView graphical programming environment with specifically designed program, which allows to receive the experimental characteristics of the reading point‘s amplitude. After the experiment, the shifts of reading point have been converted into the angular degrees of shift.

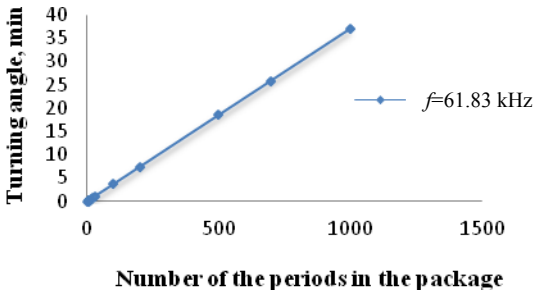

Fig. 11 Turning angle dependence on the number of periods in the package. Harmonic signal amplitude U_{RMS} = 56 V, frequency f = 61.83 kHz

For resolution investigation of the flow control device the package, which contains some number of periods of harmonic signal (U_{RMS} = 56 V, f = 61.83 kHz) was used. Shift dependence on harmonic number of signal cycles package is presented in Fig. 11.

The rotor starts to rotate after forming two harmonic signals whose amplitude U_{RMS} = 56 V and frequency f = 61.83 kHz for periods of package, the transition process ended after 12 ms from the end of the excitation package. After recalculating the displacement in turn a resolution of 0027' was received.

7. Conclusions

The construction of flow control device in which can be reached the light, gas or fluid flow throughput and high accuracy by the aid of the positioning of piezo actuator and moiré effect properties of membrane was designed and presented in this paper.

Selection of electrode configuration and the result of numerical simulation showed that the piezoceramic cylinder output link formed unsymmetrical running-wave type of oscillation with different excitation frequencies. The best operating frequency (61 kHz) was found by finite element method. Theoretical simulation results were validated by experiments.

References

1. **Uchino, K.; Giniewicz, J.** 2003. Micromechatronics, Marcel Dekker Inc, New York.
2. **Bansevicius, R.; Barauskas, R.; Kulvietis, G; Ragulskis, K.** 1988. Vibromotors for Precision Microrobots, Hemisphere Publishing Corp., USA 9.
3. **Jurenas, V.**; **Bansevicius, R.; Navickaite, S.** 2010**.** Piezoelectric bimorphs for laser shutter systems: optimization of dynamic characteristics, Mechanika 5(85): 44-47.
4. **Rahmoune, M; Osmont, D.** 2010. Classic finite elements for simulation of piezoelectric smart structures, Mechanika 6(86): 50-57.
5. **Uchino, K.** 1998. Piezoelectric ultrasonic motors: overview, Journal of Smart Materials and Structures, vol.7: 273-285.
6. **Sashida, T.; Kenjo, T.** 1994. An Introduction to Ultrasonic Motors, Oxford Press.
7. **Bansevicius, R.; Kulvietis, G.; Mazeika, D.** 2008. Piezoelectric wide range laser deflecting/scanning devices with one and two degrees-of-freedom: state of the art and latest development, Proceedings of 11th Int. Conference "Actuator 08": 117-120.
8. **Hemsel, T.; Wallaschek, J.** 2000. Survey of the present state of the art of piezoelectric linear motors, Ultrasonics, vol.38: 37-40.
9. **Friend, J.; Nakamura, K.; Ueha, S.** 2005. A traveling-wave linear piezoelectric actuator with enclosed piezoelectric elements – the "Scream" actuator, Proceedings of the 2005 IEEE/ASME International Conference on Advanced Intelligent Mechatronics Monterey, California, USA: 183-188.
10. **Bansevičius, R.P.; Mitrulevičiūtė, R.; Ragulskis, M.K.** Device of the flow control, patent application No.2007 006 / inventors: Ramutis Bansevičius, Rūta Mitrulevičiūtė, Minvydas Ragulskis; applicant: Kaunas University of Technology, 20081229. 7 p. (in Lithuanian).

R. Bansevičius, R. Rimašauskienė, D. Mažeika, G. Kulvietis

CILINDRINIO PJEZOELEKTRINIO VYKDIKLIO, NAUDOJAMO SRAUTŲ VALDYMO ĮRENGINYJE, TYRIMAS

R e z i u m ė

Šiame straipsnyje pateikiamas ir analizuojamas cilindro formos pjezoelektrinis vykdiklis, kuris naudojamas srautų valdymo įrenginių konstrukcijoje. Nesimetriniai bėgančiosios bangos tipo virpesiai sukuriami vykdiklio viršutinėje dalyje, kai jis žadinamas skirtingų fazių harmoniniais virpesiais. Pjezokeraminio elemento elektrodai žadinami sinusine įtampa, kurios fazių skirtumas $\pi/3$. Skaitmeninis modeliavimas, paremtas baigtinių elementų metodu, buvo naudojamas modaliniams dažniams bei harmonikoms analizuoti ir žiedo judėjimo trajektorijai apskaičiuoti. Skaitmeninio modeliavimo ir eksperimentinių tyrimų rezultatai pateikti publikacijoje.

R. Bansevičius, R. Rimašauskienė, D. Mažeika, G. Kulvietis

ANALYSIS OF CYLINDRICAL PIEZOELECTRIC ACTUATOR USED IN FLOW CONTROL DEVICE

S u m m a r y

A design of cylindrical type piezoelectric actuator used in the flow control systems is proposed and analyzed in the paper. Traveling wave is generated on the top area of the actuator applying harmonic oscillations with different phases. Electrodes of piezoceramic elements are excited by harmonic voltage with phase difference of $\pi/3$. Numerical modeling based on finite element method was performed to find resonant frequencies and modal shapes of the actuator and to calculate the trajectories of the upper points movements under different excitation schemes. Results of numerical and experimental studies are discussed.

Received February 15, 2011
Accepted June 30, 2011